nature astronomy

Article https://doi.org/10.1038/s41550-023-01925-x

Insight into multi-step geological evolution of C-type asteroids from Ryugu particles

In the format provided by the authors and unedited

Supplementary Figures 1–12
Supplementary Tables 1–6

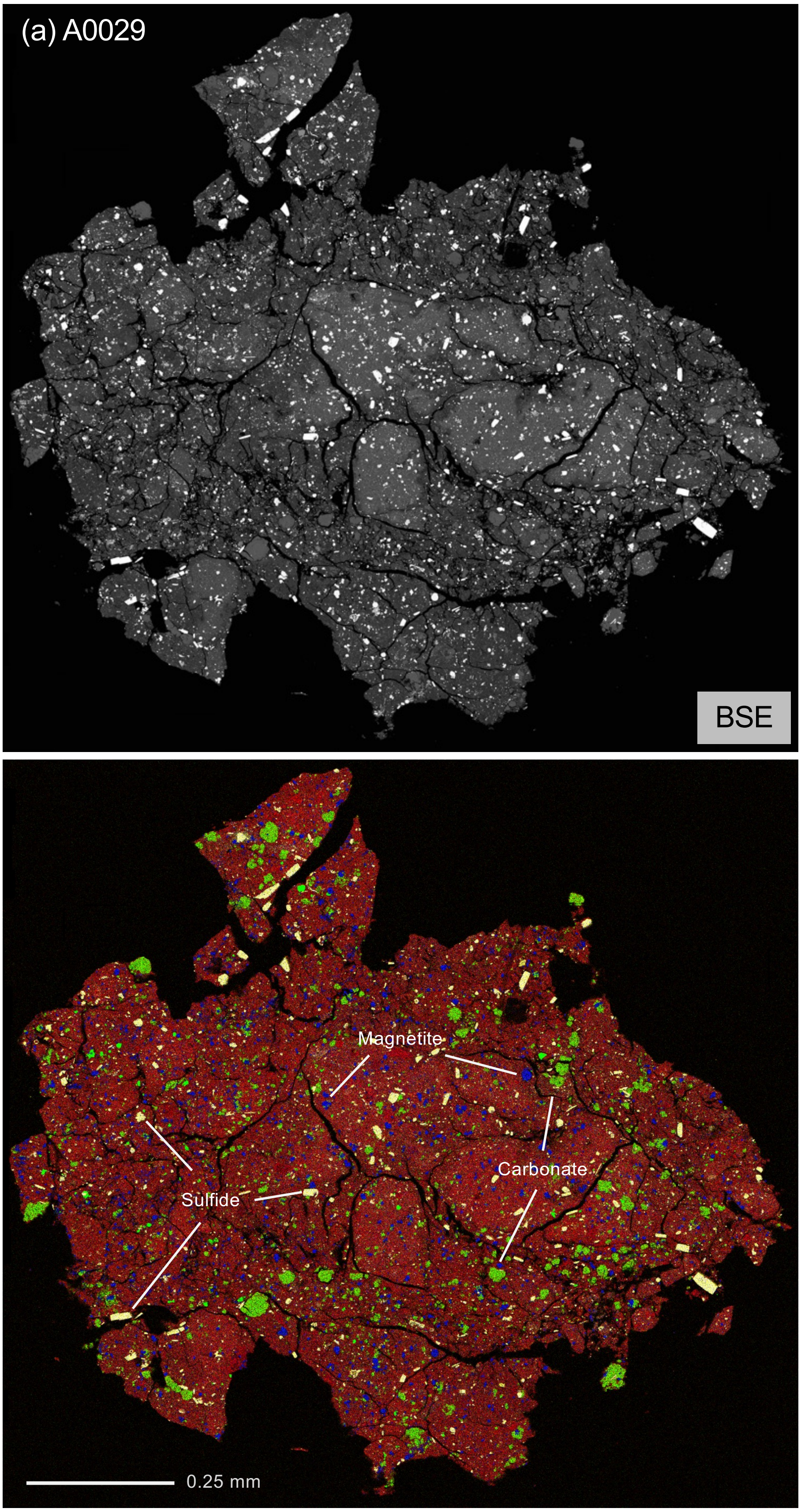

(a) A0029
BSE
Magnetite
Carbonate
Sulfide
0.25 mm

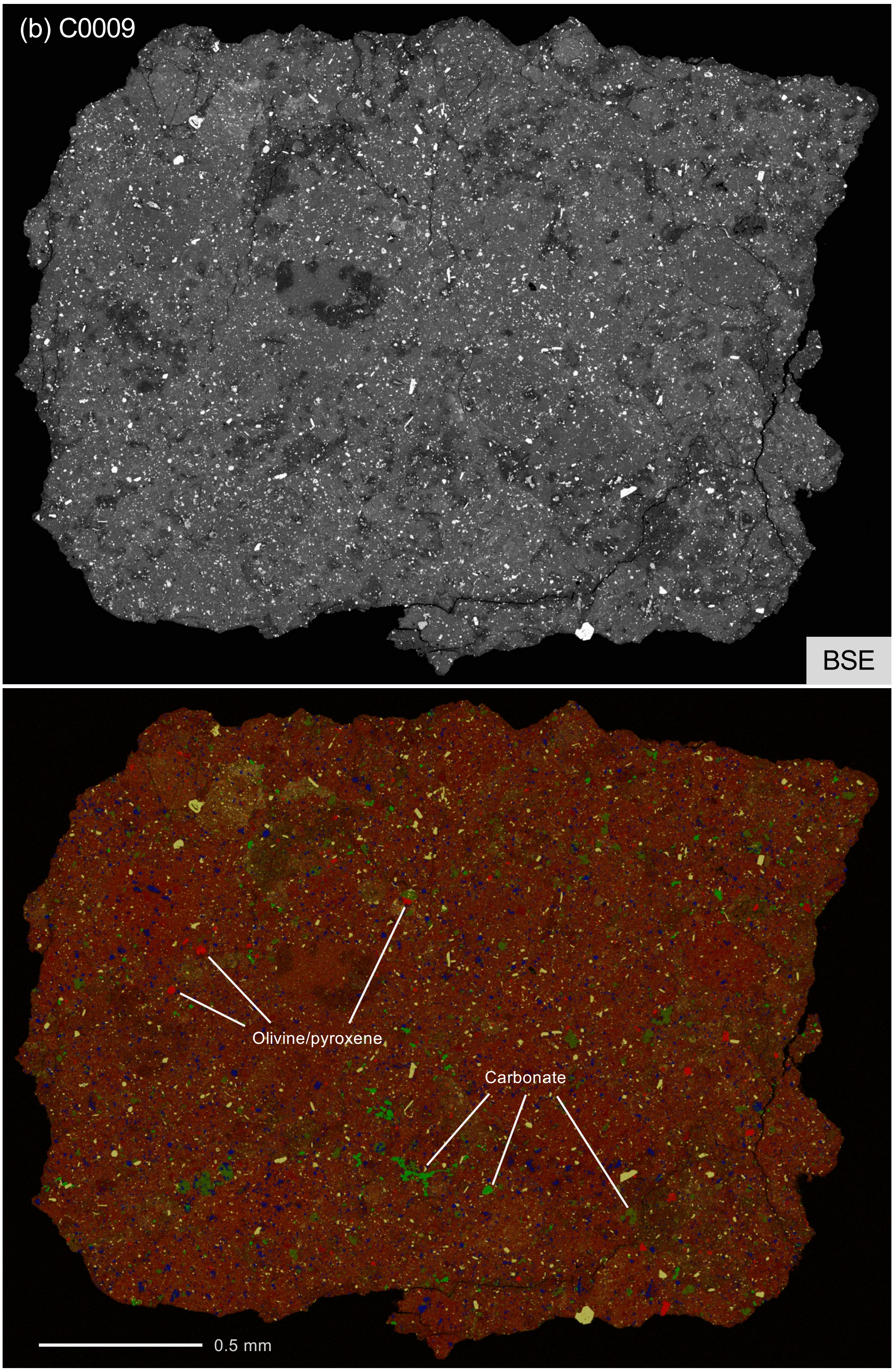

Supplementary Fig. 1. Images of polished sections. Backscattered electron (BSE) images and combined chemical maps (MgKα, CaKα, FeKα, SKα) of A0029 (a) and C0009 (b). Red: phyllosilicate-rich; green: carbonates (dolomite, Ca-rich carbonate); blue: magnetite (Mag); yellow: pyrrhotite.

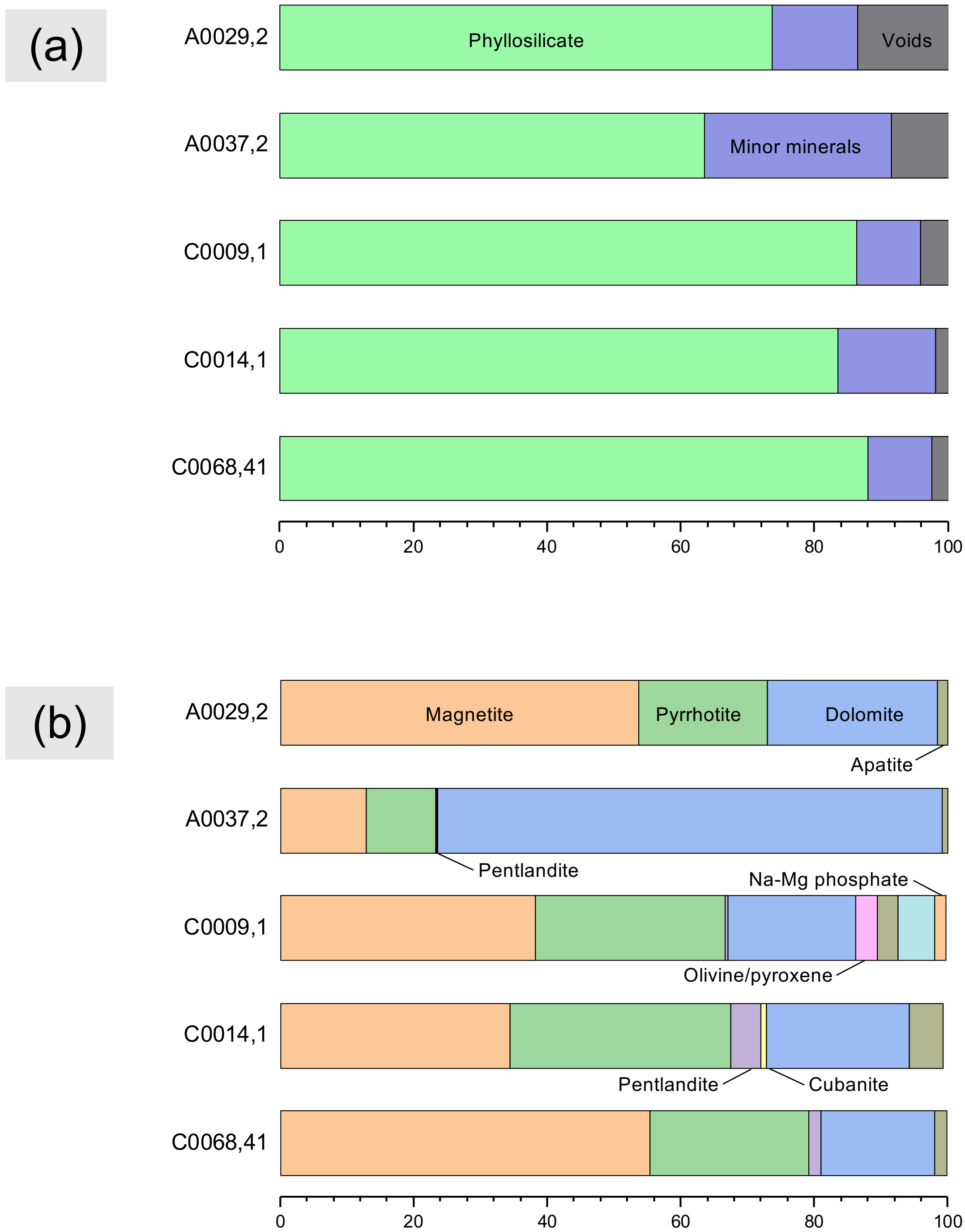

Supplementary Fig. 2. (a) Modal abundances (vol%) of phyllosilicates, minor minerals, and voids. (b) Modal abundances of minor minerals normalized to 100%.

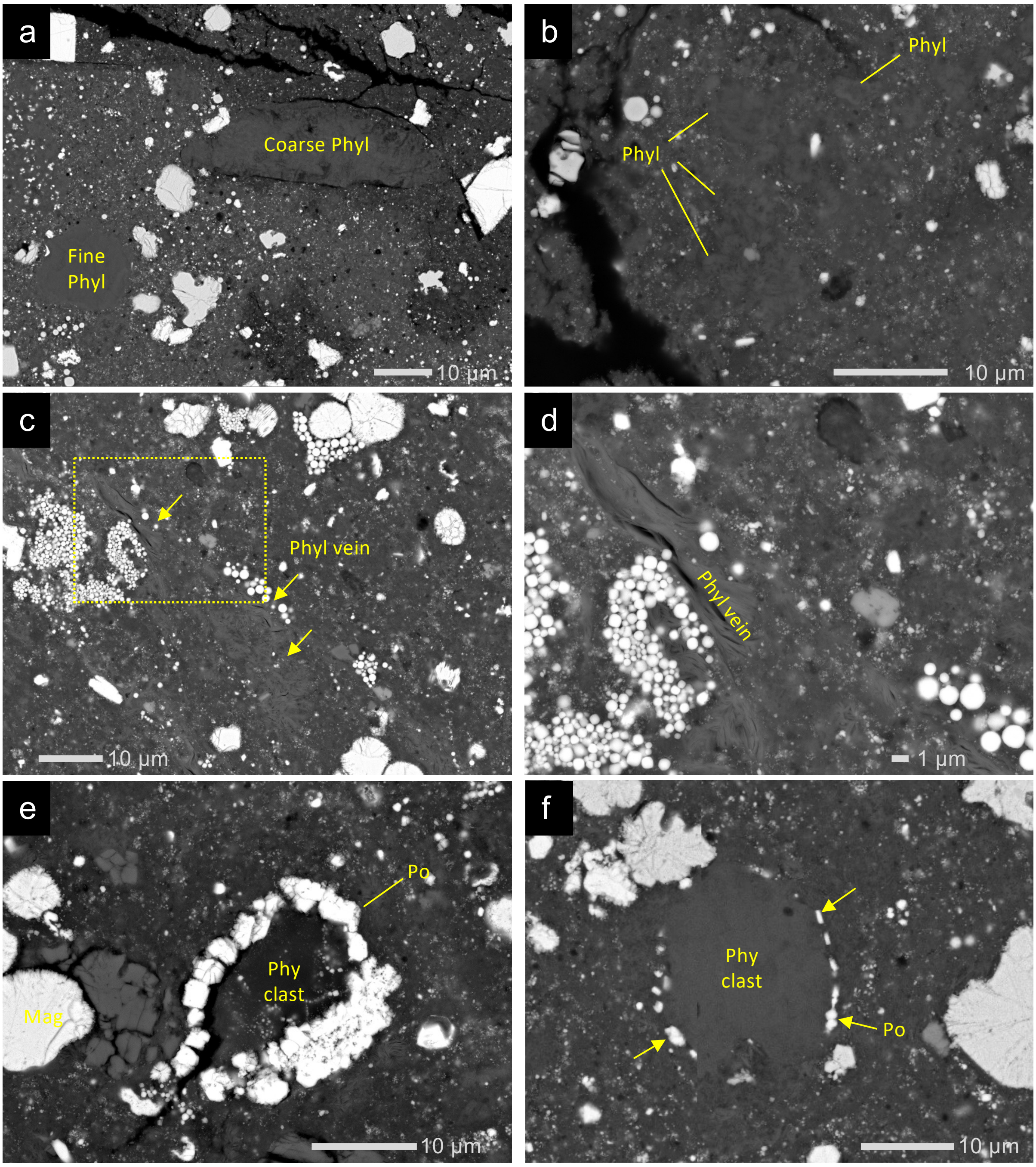

Supplementary Fig. 3. BSE images of polished sections of Ryugu particles. (a) Coarse-grained and fine-grained phyllosilicate clasts set in matrix in C0014. (b) Tiny phyllosilicate clasts. (c) Vein of phyllosilicates in C0014. (d) Enlarged view of the dotted box in (c). (e) Fragment of phyllosilicate matrix surrounded by pyrrhotite in C0068. (f) Phyllosilicate clast coated with tiny pyrrhotite grains (C0068).

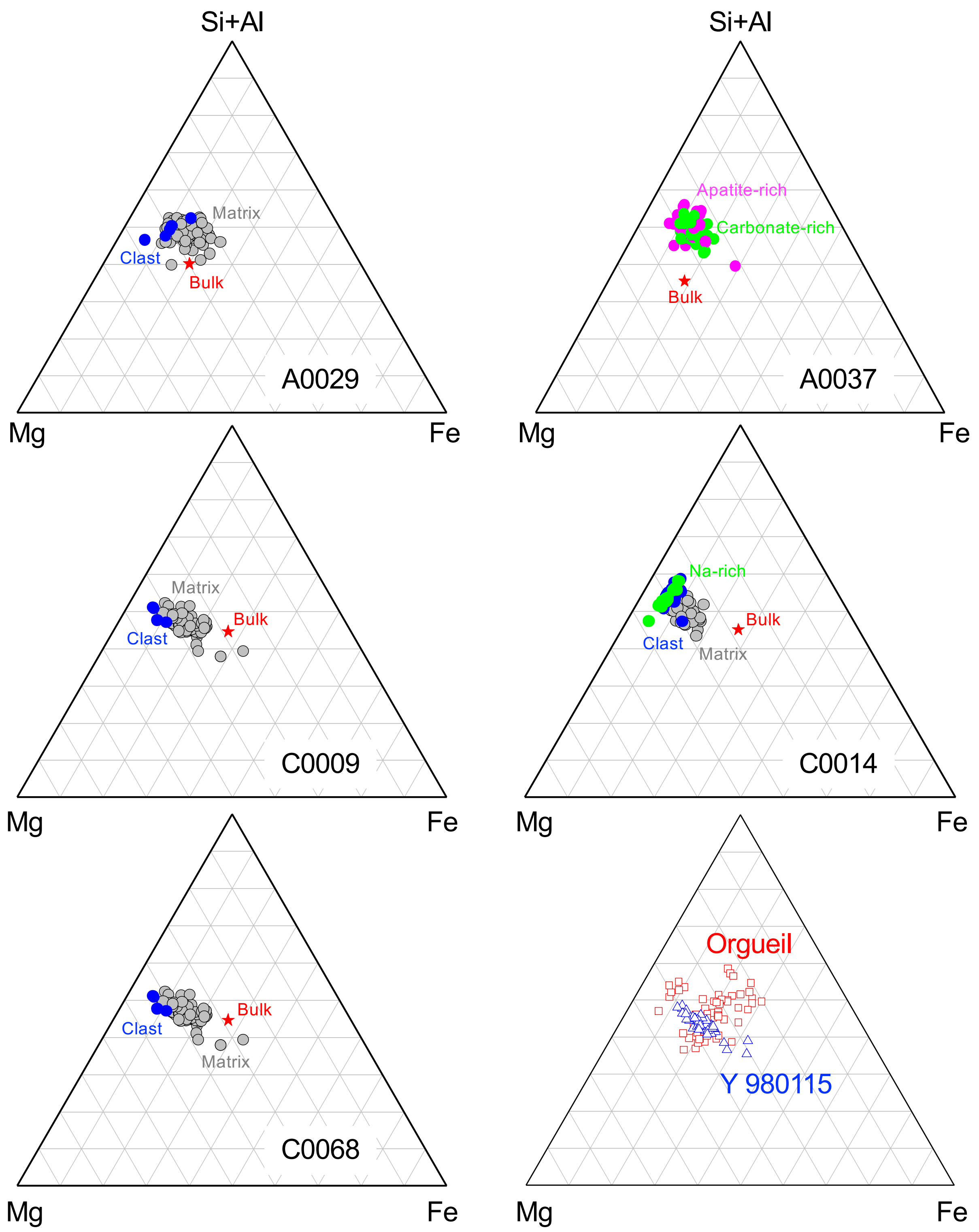

Supplementary Fig. 4. Chemical compositions of phyllosilicate clasts and matrix of Ryugu particles determined by EPMA, plotted on Si+Al – Mg – Fe (mol%) triangles. Compositions of Orgueil (CI) and Y 980115 (CY) are shown for comparison.

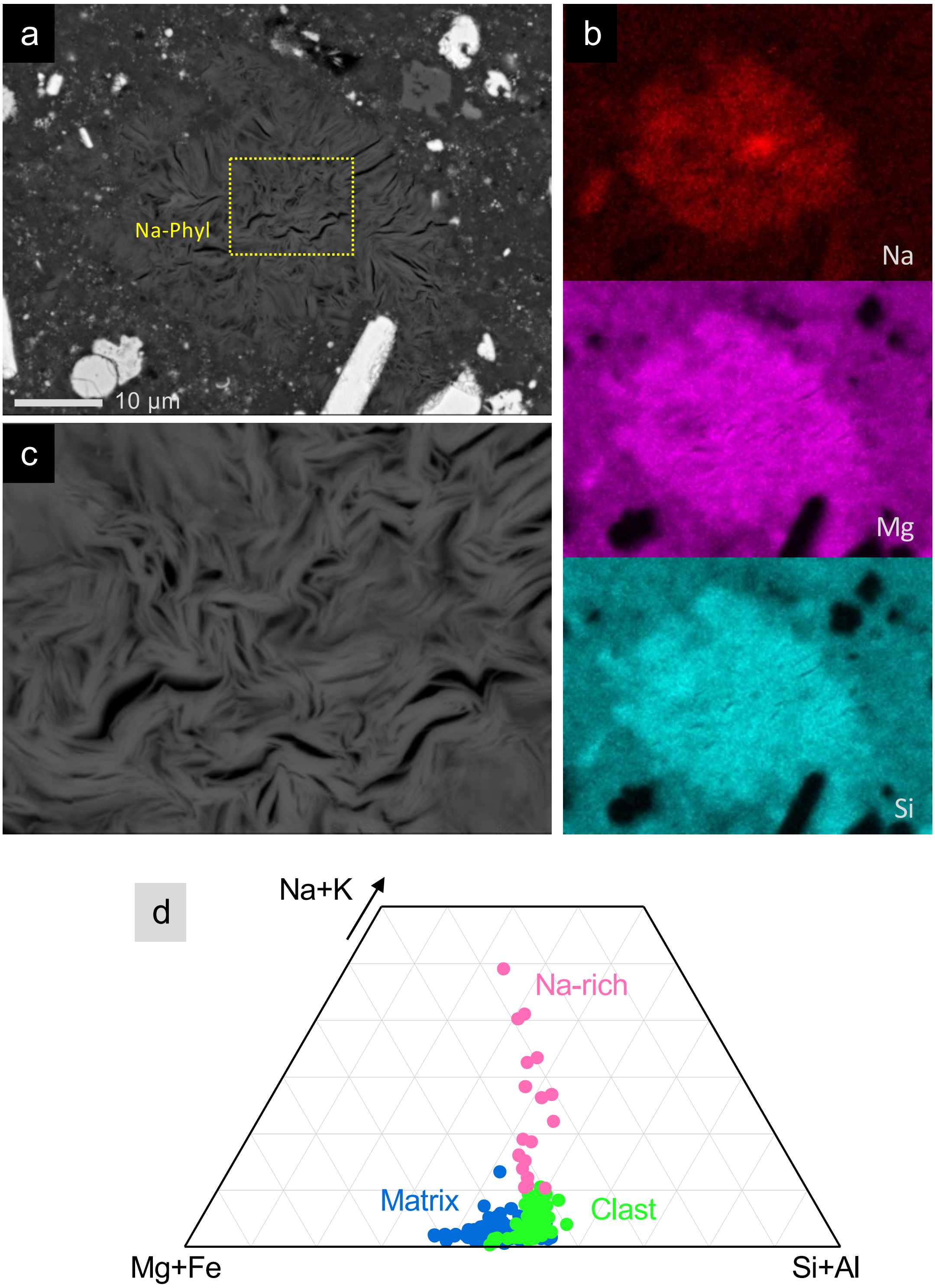

Supplementary Fig. 5. Na-rich phyllosilicate clast (Mg13) in C0014. (a) BSE image of Na-rich phyllosilicate clast in C0014. (b) X-ray maps (NaKα, MgKα, SiKα) of (a). (c) Enlarged image of the dotted square in (a). The clast shows a feathery texture similar to other Na-poor phyllosilicate clasts (c.f., Fig. 2). (d) Chemical compositions of Na-rich phyllosilicate (Na-rich), and of matrix and clasts from the other sections.

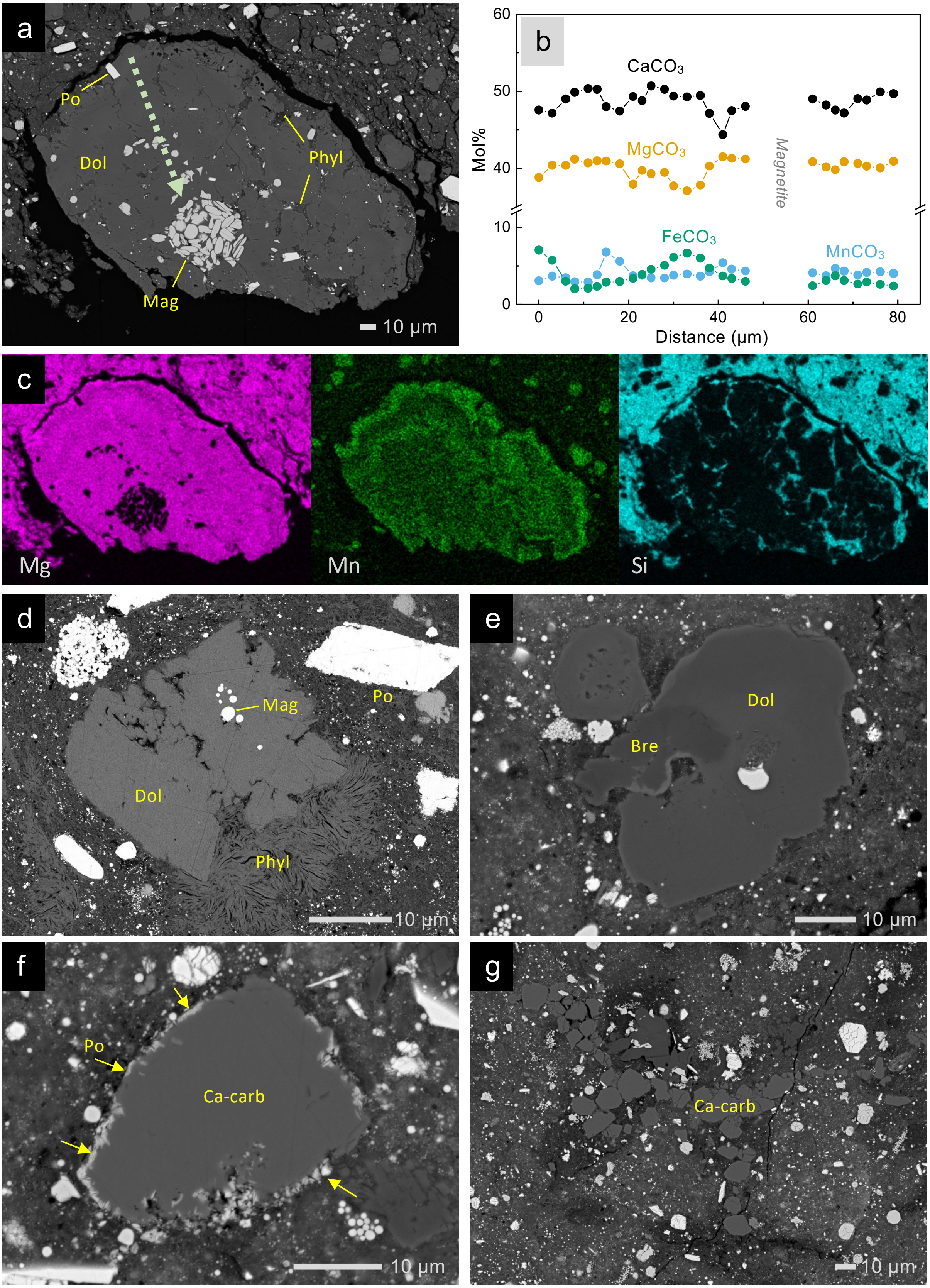
a
Po
Dol
Phyl
Mag
10 μm
b
CaCO3
MgCO3
FeCO3
MnCO3
Magnetite
Mol%
Distance (μm)
60
50
40
10
0
0
20
40
60
80
c
Mg
Mn
Si
d
Mag
Po
Dol
Phyl
10 μm
e
Dol
Bre
10 μm
f
Po
Ca-carb
10 μm
g
Ca-carb
10 μm

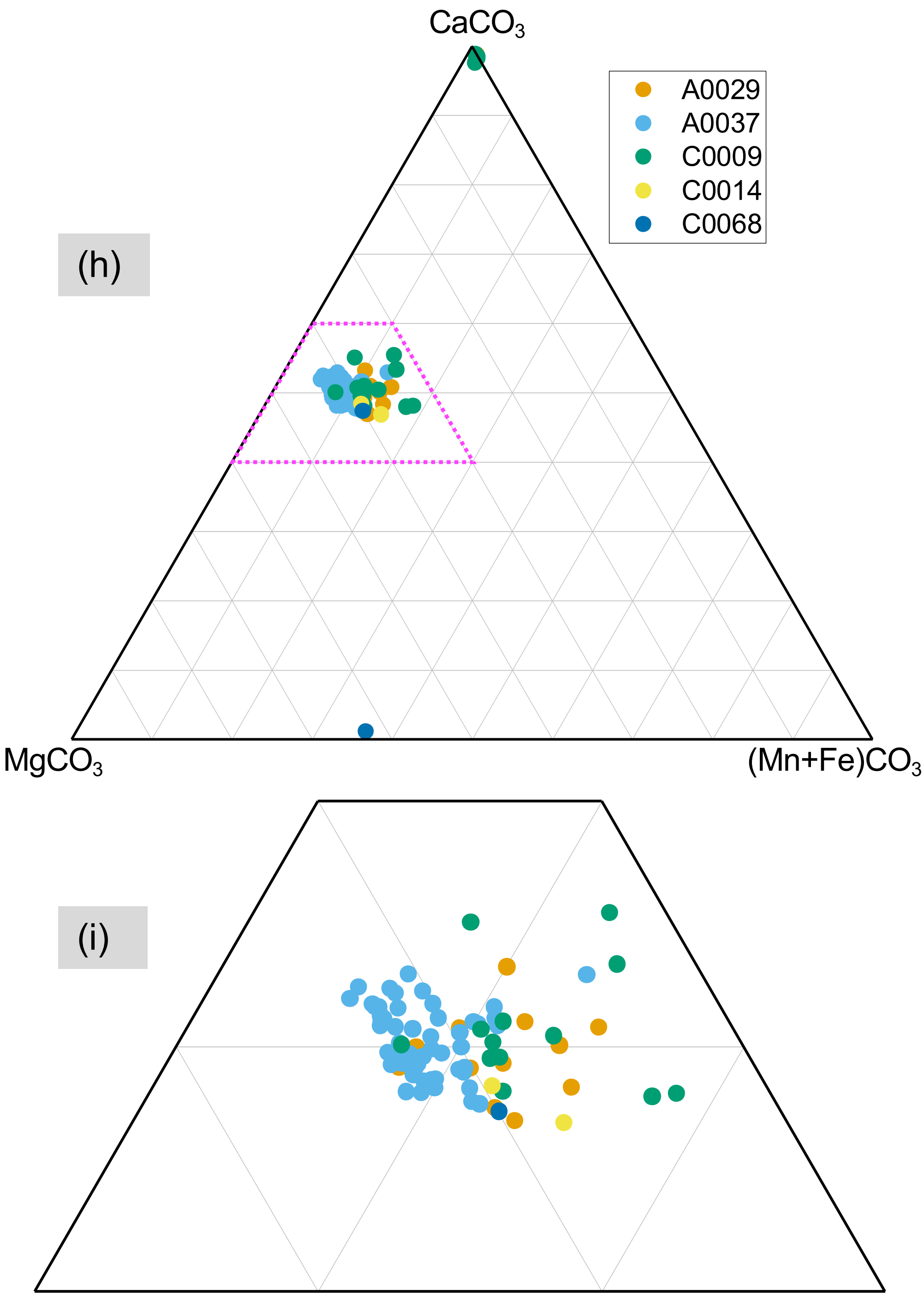

Supplementary Fig. 6. BSE images and chemical compositions of carbonates in Ryugu particles. (a) Dolomite clast in C0037, enclosing fine-grained phyllosilicate matrix (dark-gray), magnetite, and sulfide (white). (b) Zoning profiles of the dolomite across a dotted line in (a). (c) Chemical maps (MgKα, MnKα and SiKα) of dolomite (a). (d) BSE image of dolomite in sharp contact with coarse-grained phyllosilicate. (e) Dolomite contacted with breunnerite. (f) Ca-carbonate ("Ca2") surrounded by thin rims of pyrrhotite. (g) Chain of Ca-carbonte grains. (h) Chemical compositions of carbonate. (i) Enlarged figure of a dotted trapezoidal box in (h).

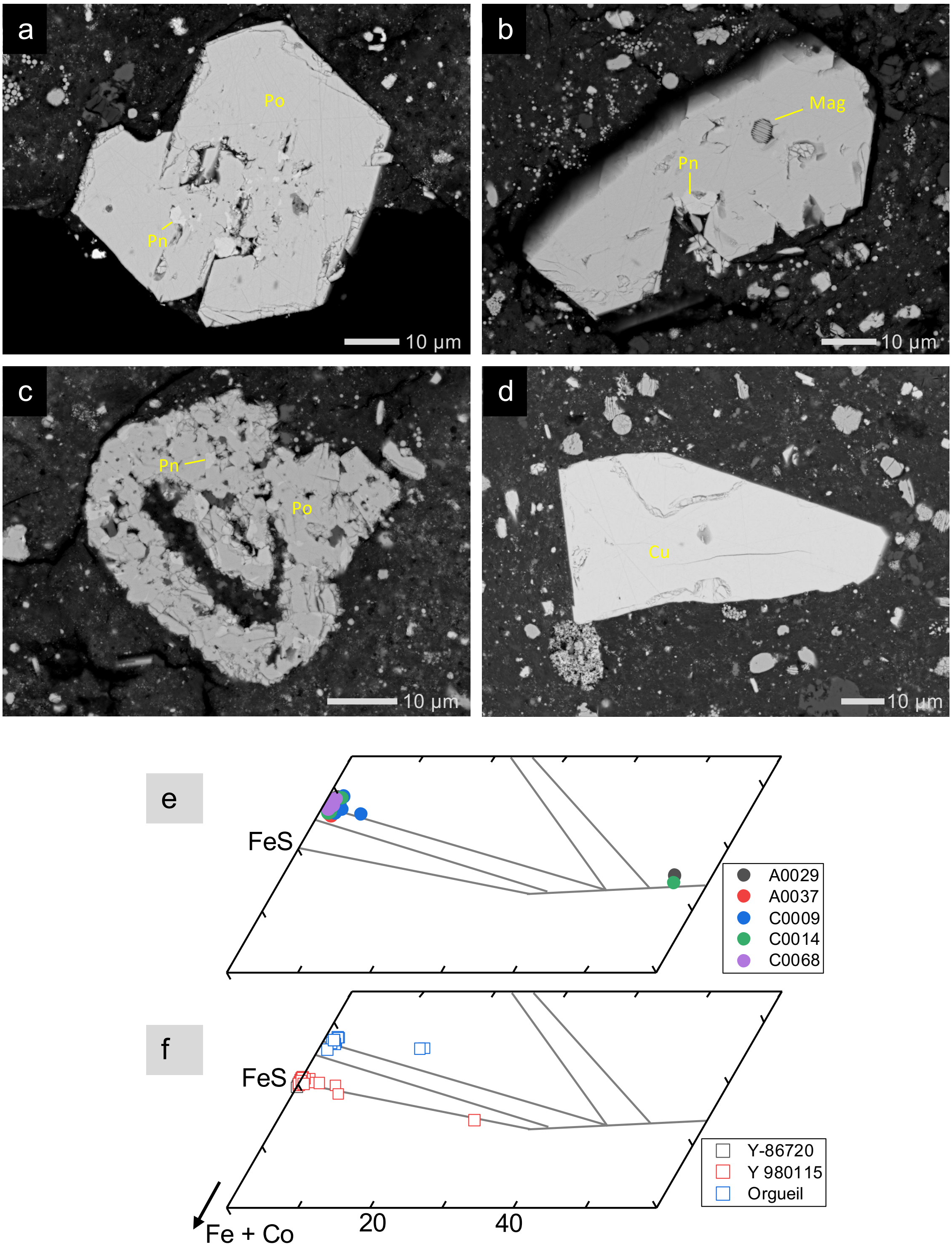

Supplementary Fig. 7. BSE images and chemical compositions of sulfide minerals. (a) Euhedral (hexagonal) grain of pyrrhotite (Po) in C0009. (b) Inclusion of platelet magnetite in pyrrhotite fragment (A0037). (c) A subrounded aggregate of pyrrhotite. There are tiny pentlandite inclusions (Pn, white). (d) Blocky grain of cubanite in C0014. (e) Chemical compositions of sulfides of the Ryugu particles plotted on the 100–135 °C phase diagram[34]. (f) Chemical compositions of sulfides of Orgueil (CI), Y-86720 (CY) and Y 980115 (CY) for comparison.

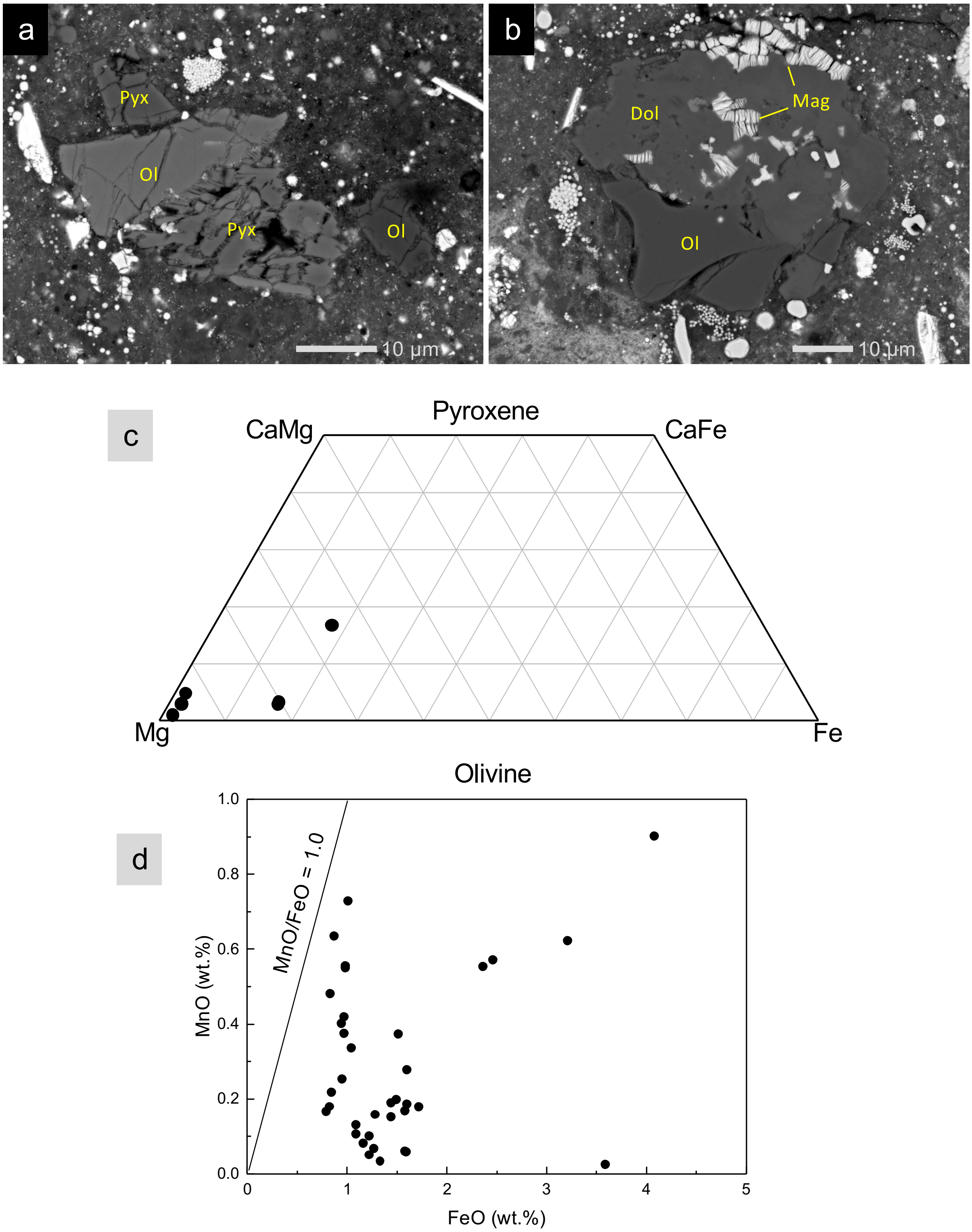

Supplementary Fig. 8. BSE images and chemical compositions of anhydrous silicates (olivine and pyroxene) in C0009 Ryugu particles. (a) An assemblage of olivine (Ol), low- and high-Ca pyroxene (Pyx). (b) Olivine in sharp contact with dolomite (Dol). (c) Pyroxene compositions plotted on a pyroxene quadrilateral. Ca-rich pyroxene may have been derived from chondrules. (d) FeO vs. MgO of olivine.

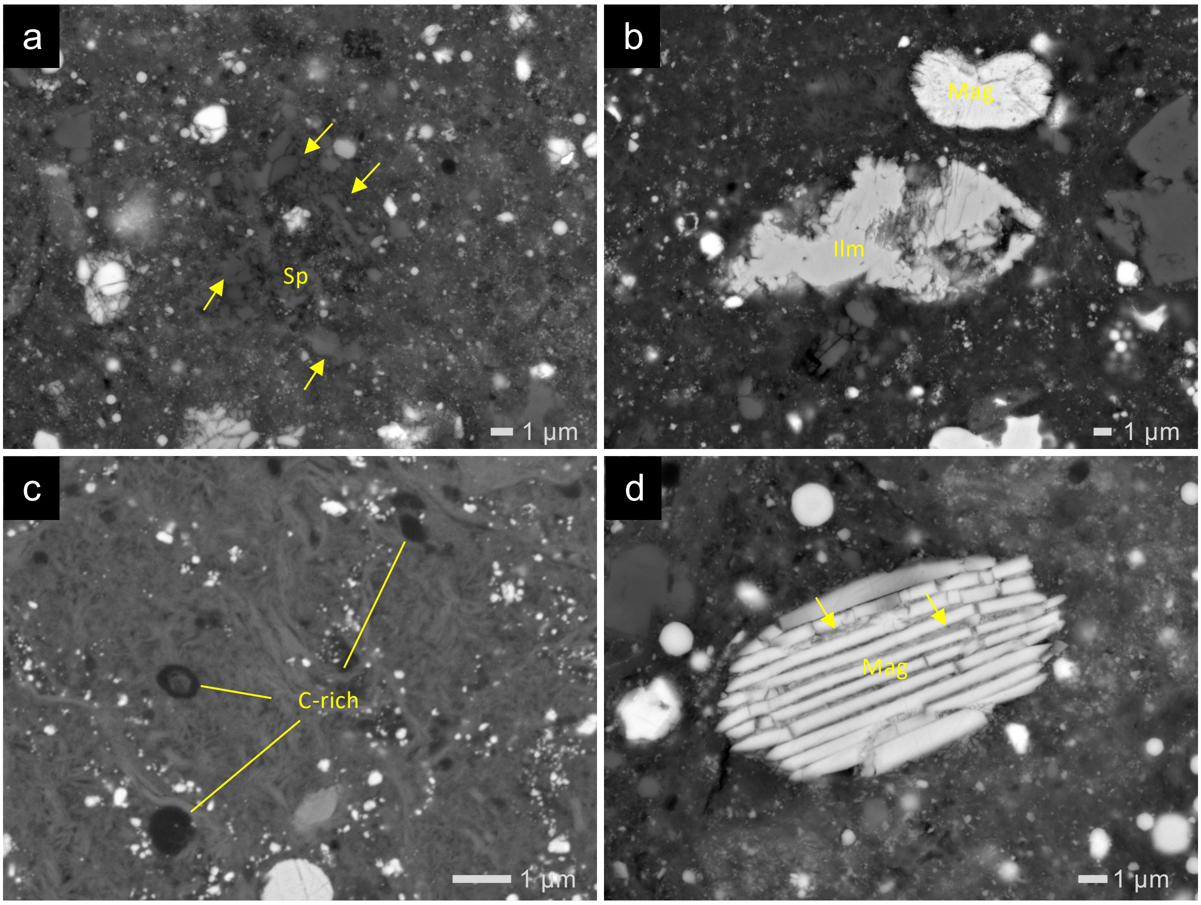

Supplementary Fig. 9. BSE images of polished sections of Ryugu particles. (a) An assemblage of fine-grained spinel grains (Sp, arrows) in C0009. (b) Ilmenite grain in C0014, which is fractured and corroded. (c) C-rich phases (dark-gray) in A0014 which were scattered in a fine-grained phyllosilicate-rich matrix. (d) Platelet magnetite (Mag) in C0009, which is partly corroded (yellow arrows).

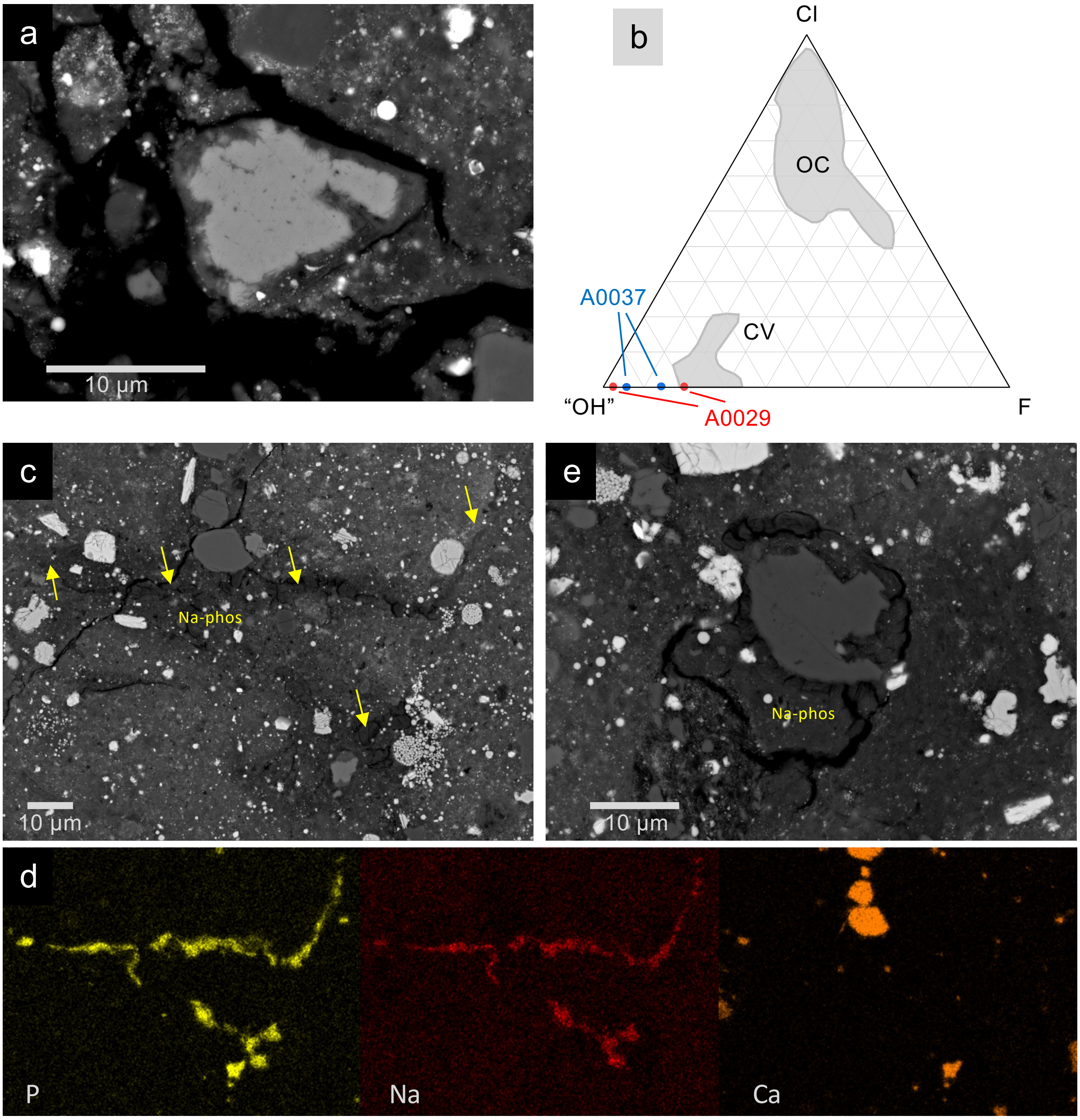

Supplementary Fig. 10. Phosphates in Ryugu particles. (a) BSE image of apatite in C0029. Apatite shows an irregular shape indicating corrosion. (b) Chemical compositions of apatite in Ryugu particles (A0029, A0037). The areas of other chondrites are from Piralla et al. (2021)[44]. (c) BSE image of Na-rich phosphate (dark-gray, arrows, "Na-phos") in C0009 forming veins. (d) Chemical maps (PKα, NaKα, CKα) of (c). (e) BSE image of Na-rich phosphate partially surrounds a dolomite grain.

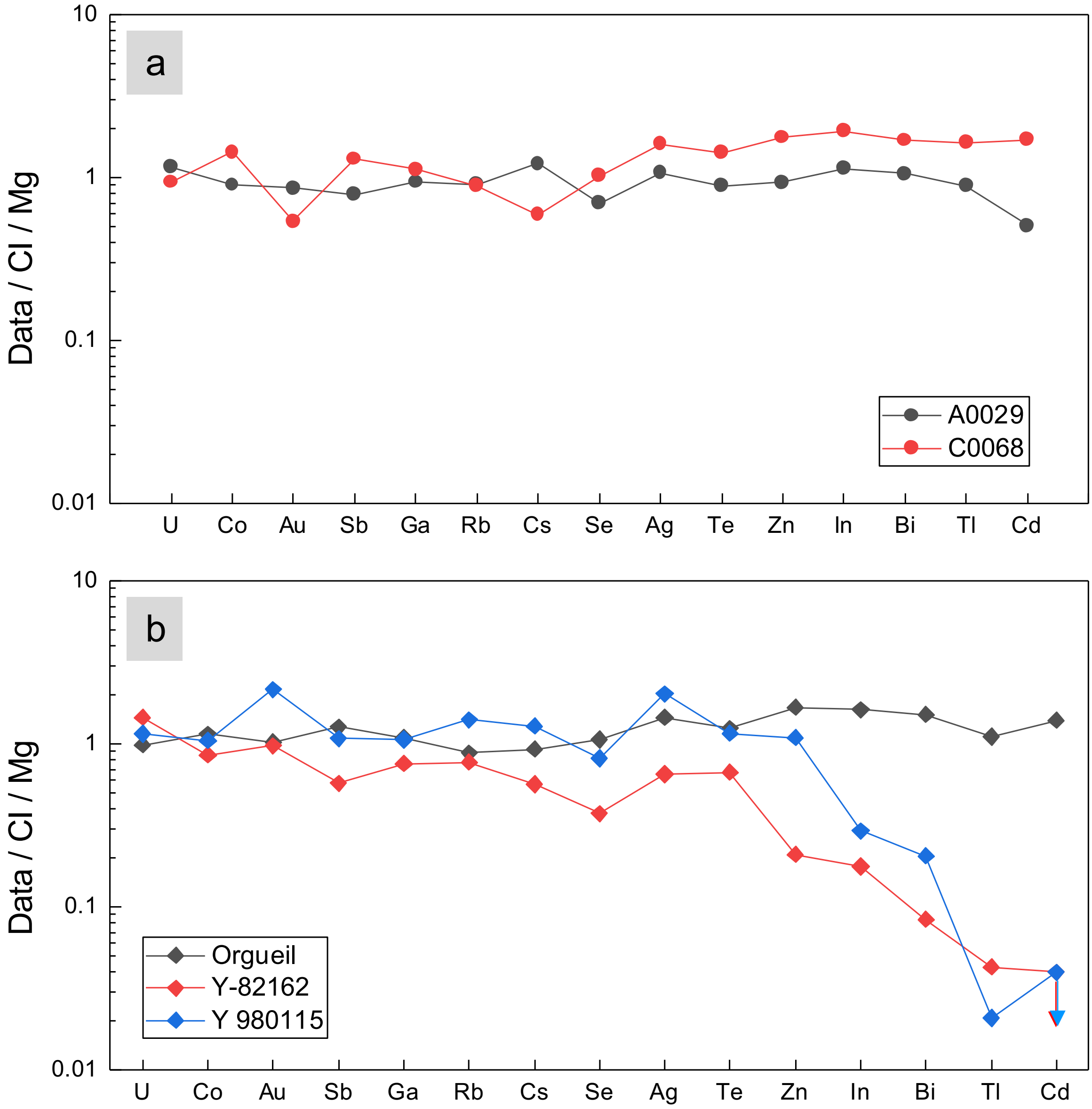

Supplementary Fig. 11. Chemical compositions of the particles, A0029, and A0068 determined by LA-ICP-MS, normalized to CI chondrites[14] and Mg. The data of Orgueil, Y-82162, and Y 980115 (CY) are shown for comparison. Arrows refer to the detection limits.

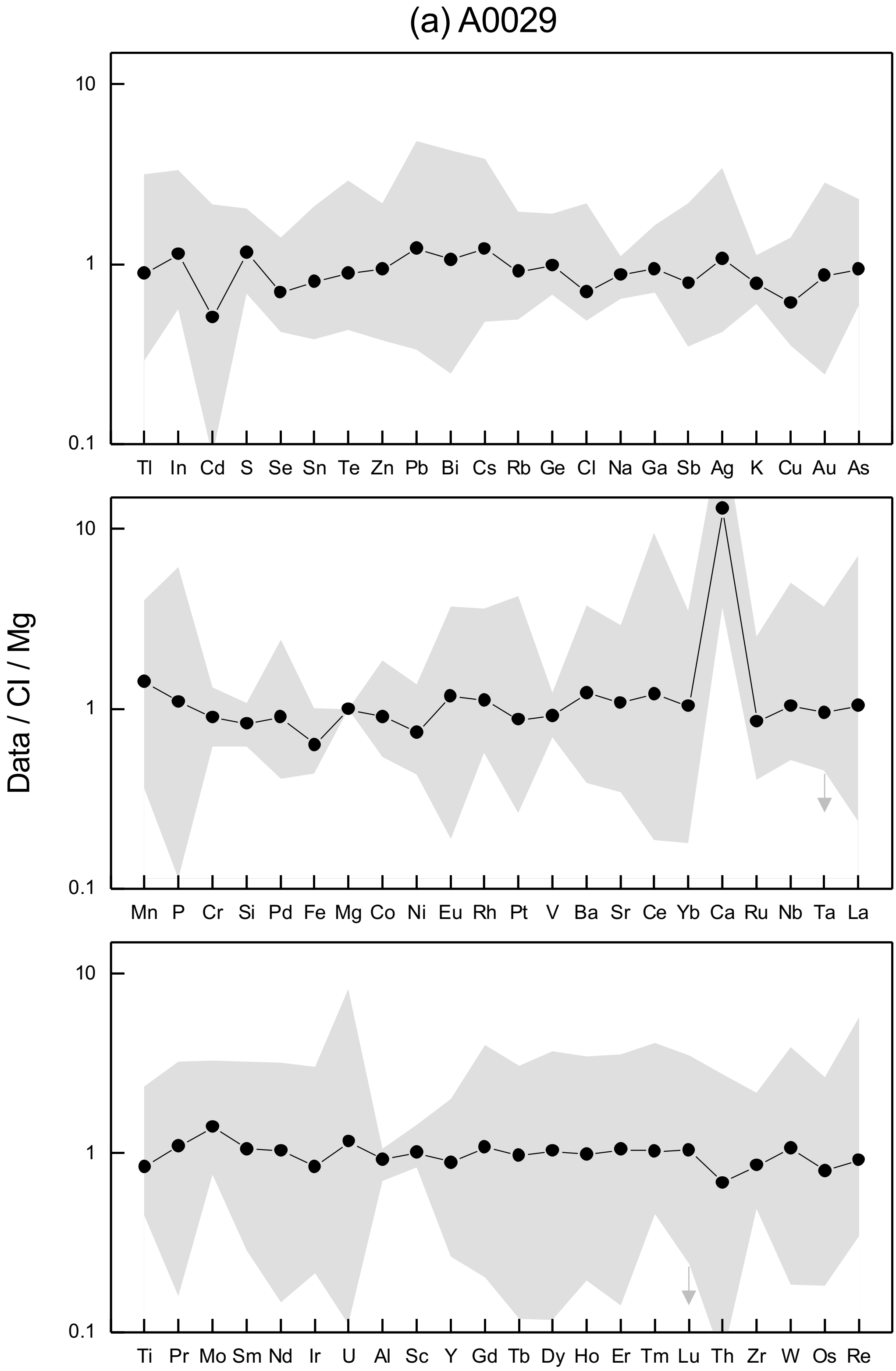
(a) A0029
Data / CI / Mg
10
1
0.1
Tl In Cd S Se Sn Te Zn Pb Bi Cs Rb Ge Cl Na Ga Sb Ag K Cu Au As
Mn P Cr Si Pd Fe Mg Co Ni Eu Rh Pt V Ba Sr Ce Yb Ca Ru Nb Ta La
Ti Pr Mo Sm Nd Ir U Al Sc Y Gd Tb Dy Ho Er Tm Lu Th Zr W Os Re

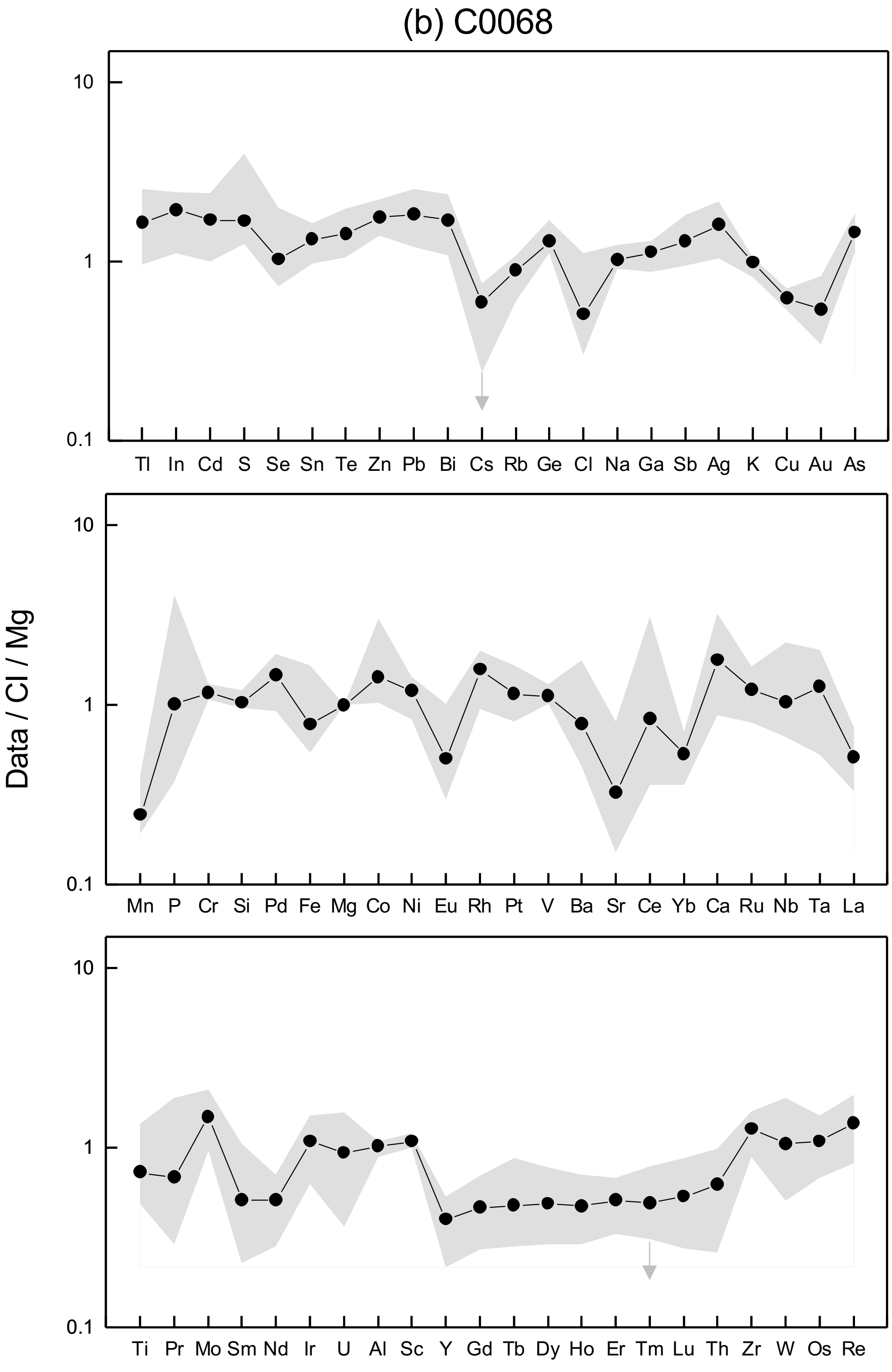

Supplementary Fig. 12. Chemical compositions of A0029 (a) and C0068 (b) determined by LA-ICP-MS analyses, normalized to Mg and CI chondrites[14]. Gray shades refer to compositional ranges of each sweep.

Supplementary Table 1. Representative chemical compositions of phyllosilicates (wt%) determined by EPMA.

	SiO_2	Al_2O_3	K_2O	Na_2O	CaO	FeO	MgO	MnO	Cr_2O_3	TiO_2	NiO	ZnO	P_2O_5	SO_3	Cl	Total	Mg#
A0029																	
Clast	40.0	1.66	0.08	1.08	0.02	13.8	17.9	0.21	1.38	0.09	0.09	<0.1	0.11	1.43	0.09	78.0	69.9
	37.5	1.04	0.04	0.12	0.02	6.44	26.2	<0.08	0.21	<0.05	0.11	<0.1	<0.07	<0.11	0.04	71.9	87.9
Matrix	21.8	1.24	0.04	0.39	0.11	6.06	11.2	<0.08	0.26	<0.05	0.68	<0.1	<0.07	6.41	0.18	48.4	76.7
A0037																	
Clast	29.7	1.76	0.08	0.93	0.10	8.03	15.6	<0.08	0.38	<0.05	0.79	0.12	<0.07	7.11	0.04	64.8	77.6
	27.6	1.37	0.06	0.82	0.05	8.55	15.9	<0.08	0.30	0.07	0.76	<0.1	<0.07	4.72	0.08	60.4	76.8
C0009																	
Clast	44.7	2.53	0.12	0.81	<0.02	7.33	26.9	0.09	0.44	0.14	0.15	<0.1	<0.07	0.31	0.09	83.7	86.8
	28.6	1.72	0.06	0.62	0.04	11.5	15.8	<0.08	0.39	0.05	0.84	0.13	<0.07	9.62	0.09	69.6	70.9
Matrix	38.9	2.40	0.02	0.59	<0.02	11.9	24.8	0.16	0.53	0.06	0.10	<0.1	<0.07	0.92	0.13	80.4	78.8
C0014																	
Clast	41.0	3.48	0.03	0.38	0.05	14.8	25.5	0.24	0.69	<0.05	0.22	<0.1	<0.07	1.07	0.05	87.5	75.4
	44.3	3.21	0.10	0.57	0.02	8.71	20.9	<0.08	0.38	<0.05	1.08	<0.1	<0.07	5.97	0.05	85.4	81.1
Na-rich	30.8	3.30	0.26	36.2	<0.02	4.52	23.4	<0.08	0.07	<0.05	0.12	<0.1	<0.07	<0.11	0.02	98.8	90.2
Matrix	43.8	3.93	0.09	3.69	<0.02	6.54	25.7	<0.08	0.43	<0.05	0.10	0.12	<0.07	0.12	0.01	84.6	87.5
C0068																	
Clast	27.6	1.42	0.05	0.59	<0.02	10.0	16.2	0.12	0.36	0.07	1.26	<0.1	<0.07	8.36	0.04	66.1	74.2
	25.3	0.79	0.04	0.62	0.13	8.94	8.79	<0.08	0.72	0.09	<0.06	<0.1	<0.07	0.78	0.03	46.4	63.7
Matrix	46.5	4.25	0.13	1.18	<0.02	6.55	26.5	<0.08	0.46	<0.05	<0.06	<0.1	<0.07	0.17	0.02	85.9	87.8

Supplementary Table 2. Chemical compositions (wt%) of carbonates determined by EPMA.

	SiO_2	Al_2O_3	MgO	FeO	CaO	MnO	Na_2O	Cl	Cr_2O_3	Total	$CaCO_3$	$MgCO_3$	$FeCO_3$	$MnCO_3$	
Dolomite															
A0029															
11	0.38	0.05	16.9	2.95	27.1	5.12	0.05	<0.01	<0.05	52.5	48.4	35.3	4.8	8.3	
20	0.11	<0.02	19.2	3.53	27.1	1.55	<0.02	0.02	0.06	51.6	48.4	40.2	5.7	2.5	
A0037															
45	0.28	<0.02	18.7	2.35	25.8	4.73	<0.02	<0.01	<0.05	51.8	46.0	39.0	3.8	7.7	
54	<0.05	<0.02	19.7	1.82	27.9	1.24	<0.02	<0.01	<0.05	50.7	49.9	41.2	2.9	2.0	
28	<0.05	<0.02	19.1	2.35	25.9	3.55	<0.02	0.01	<0.05	51.0	46.2	39.9	3.8	5.7	*
29	<0.05	<0.02	19.3	2.38	26.3	2.54	0.05	0.02	<0.05	50.6	47.0	40.4	3.8	4.1	*
32	<0.05	<0.02	19.2	2.42	26.2	2.47	<0.02	<0.01	<0.05	50.3	46.7	40.1	3.9	4.0	*
35	<0.05	<0.02	18.8	2.51	27.9	1.42	0.11	0.02	<0.05	50.8	49.8	39.4	4.1	2.3	*
39	<0.05	<0.02	18.8	1.87	26.7	3.49	0.03	<0.01	<0.05	50.9	47.7	39.3	3.0	5.7	*
40	<0.05	<0.02	18.7	2.38	28.7	1.64	0.08	<0.01	<0.05	51.4	51.2	39.0	3.8	2.7	*
42	<0.05	<0.02	19.0	2.57	26.6	2.71	0.06	0.03	<0.05	50.9	47.4	39.7	4.1	4.4	*
49	<0.05	<0.02	19.5	2.56	26.9	2.31	<0.02	0.02	<0.05	51.4	48.1	40.8	4.1	3.7	*
50	0.46	0.03	18.9	1.96	26.1	3.24	0.05	0.01	<0.05	50.9	46.7	39.6	3.2	5.3	*
63	0.06	<0.02	18.0	2.34	27.7	3.77	<0.02	<0.01	<0.05	51.9	49.4	37.7	3.8	6.1	*
82	<0.05	<0.02	19.6	2.49	27.9	1.47	<0.02	<0.01	<0.05	51.4	49.7	40.9	4.0	2.4	*
86	<0.05	<0.02	17.6	2.11	27.7	4.26	0.03	<0.01	0.08	51.8	49.4	36.9	3.4	6.9	*
91	<0.05	<0.02	18.7	2.66	26.6	3.58	<0.02	<0.01	<0.05	51.6	47.4	39.2	4.3	5.8	*
94	0.42	0.05	19.5	2.83	26.0	2.91	<0.02	<0.01	<0.05	51.8	46.5	40.9	4.6	4.7	*
96	0.38	<0.02	18.6	2.50	26.0	4.17	0.12	0.03	0.08	52.0	46.5	39.0	4.0	6.8	*
100	0.25	<0.02	18.9	2.48	26.3	2.42	0.03	<0.01	<0.05	50.5	47.0	39.6	4.0	3.9	*

C0009															
107	<0.05	<0.02	15.6	4.47	26.4	6.80	<0.02	<0.01	0.06	53.3	47.1	32.6	7.2	11.0	
113	<0.05	<0.02	19.2	3.26	26.8	1.42	0.15	<0.01	0.06	51.0	47.9	40.2	5.3	2.3	
103	<0.05	<0.02	17.1	1.78	29.7	2.90	0.03	<0.01	<0.05	51.5	53.0	35.7	2.9	4.7	*
C0014															
122	<0.05	<0.02	17.8	4.69	25.8	4.57	<0.02	0.03	0.12	53.1	46.1	37.3	7.6	7.4	
C0068															
127	0.17	<0.02	18.0	2.40	25.0	5.00	0.11	<0.01	<0.05	50.6	44.6	37.6	3.9	8.1	
Ca-carbonate															
C0009															
101	<0.05	0.04	0.04	0.69	54.2	0.02	0.07	<0.01	<0.05	55.1	96.7	0.1	1.1	0.0	*
102	<0.05	0.03	0.04	0.81	53.6	<0.02	0.04	<0.01	<0.05	54.5	95.6	0.1	1.3	0.0	*
105	<0.05	0.03	0.08	0.94	53.5	<0.02	0.17	<0.01	0.09	54.8	95.4	0.2	1.5	0.0	*
Breunnerite															
C0068															
129	0.98	0.08	28.86	13.65	0.60	7.92	0.07	<0.01	<0.05	52.2	1.1	60.4	22.0	12.8	

*Data used for calibration of Mn-Cr ages presented by McCain/Matsuda et al. (2023)[18].

Supplementary Table 3. Chemical compositions of sulfides (wt%) determined by EPMA.

	Fe	S	Ni	Co	Cr	P	Cu	Si	Mg	Al	Zn	Total
Pyrrhotite												
A0029												
36	58.8	39.3	1.08	0.05	0.03	<0.005	0.04	0.02	<0.004	<0.004	0.09	99.3
A0037												
125	58.2	39.2	0.93	0.06	0.08	0.041	<0.01	0.03	0.04	0.008	<0.02	98.6
C0009												
162	58.2	38.6	0.88	0.13	0.05	<0.005	<0.01	0.06	0.05	<0.004	0.10	98.1
C0014												
23	58.6	38.6	1.00	0.07	0.02	0.037	0.01	0.01	0.02	<0.004	0.11	98.5
C0068												
154	58.1	39.0	0.86	0.08	0.04	<0.005	<0.01	0.06	<0.004	<0.004	0.08	98.2
Pentlandite												
A0029												
39	28.1	33.2	34.8	1.98	0.06	<0.005	0.06	0.10	0.07	<0.004	<0.02	98.4
C0014												
17	28.5	32.7	35.0	1.88	0.03	<0.005	<0.01	0.05	0.03	<0.004	<0.02	98.2
Cubanite												
C0014												
11	39.9	34.9	0.01	0.02	<0.006	0.052	22.4	0.01	<0.004	<0.004	<0.02	97.4
C0014												
15	40.5	34.9	0.06	0.02	0.04	0.045	21.8	0.05	0.02	<0.004	<0.02	97.4

Supplementary Table 4. Chemical compositions (wt%) of olivine, pyroxene, magnetite, ilmenite, and spinel determined by EPMA.

	SiO_2	Al_2O_3	CaO	FeO	MgO	MnO	Cr_2O_3	TiO_2	V_2O_3	ZnO	NiO	Na_2O	Total	Mg#
Olivine														
C0009														
16	42.3	0.05	0.22	1.09	55.5	0.13	0.43	<0.02	<0.02	0.02	0.04	<0.01	99.8	98.9
17	42.2	0.06	0.20	1.09	55.5	0.11	0.42	<0.02	0.03	<0.02	0.06	<0.01	99.7	98.9
24	42.5	0.01	0.19	1.58	55.4	0.17	0.50	0.04	<0.02	<0.02	0.03	<0.01	100.4	98.4
29	42.5	0.02	0.06	0.83	56.0	0.48	0.29	0.04	<0.02	<0.02	0.07	0.01	100.3	99.2
30	42.7	0.19	0.04	0.82	56.3	0.18	0.23	0.02	<0.02	<0.02	0.06	<0.01	100.5	99.2
31	42.1	0.03	0.05	0.98	55.8	0.55	0.30	<0.02	<0.02	<0.02	0.04	<0.01	99.8	99.0
34	42.7	0.02	0.19	1.49	55.9	0.20	0.42	0.04	<0.02	<0.02	0.07	<0.01	101.1	98.5
40	42.5	0.08	0.29	1.58	55.9	0.06	0.37	0.04	<0.02	<0.02	<0.02	<0.01	100.8	98.4
42	43.0	<0.01	0.08	0.97	56.6	0.42	0.29	<0.02	0.09	<0.02	0.07	<0.01	101.5	99.0
44	42.8	0.02	0.20	1.22	55.9	0.10	0.35	0.03	<0.02	<0.02	0.06	<0.01	100.7	98.8
45	42.5	0.08	0.25	1.22	56.2	0.05	0.16	<0.02	<0.02	<0.02	0.06	<0.01	100.6	98.8
46	43.6	0.01	0.03	1.04	56.7	0.34	0.29	<0.02	<0.02	<0.02	0.05	<0.01	102.1	99.0
47	42.8	0.05	0.01	0.79	56.7	0.17	0.15	<0.02	<0.02	<0.02	0.08	0.02	100.8	99.2
49	42.4	0.02	0.05	1.01	55.4	0.73	0.34	<0.02	<0.02	<0.02	0.04	0.01	99.9	99.0
50	41.6	0.04	0.05	0.98	53.4	0.56	0.38	<0.02	<0.02	<0.02	0.07	0.01	97.1	99.0
51	42.7	0.04	0.22	1.28	55.9	0.16	0.43	<0.02	<0.02	<0.02	0.06	<0.01	100.8	98.7
53	42.7	0.14	0.24	1.72	55.9	0.18	0.52	0.06	<0.02	<0.02	0.05	0.01	101.6	98.3
54	42.5	0.01	0.04	0.97	56.2	0.38	0.41	<0.02	<0.02	<0.02	0.07	<0.01	100.5	99.0
56	42.4	0.02	0.16	1.51	55.2	0.37	0.72	<0.02	<0.02	<0.02	0.05	<0.01	100.5	98.5
61	42.6	0.02	0.19	1.44	55.6	0.15	0.54	0.04	<0.02	0.03	0.04	<0.01	100.7	98.6
62	42.5	0.03	0.09	0.94	56.3	0.40	0.34	<0.02	<0.02	<0.02	<0.02	<0.01	100.6	99.1

57	38.1	<0.01	0.11	25.61	37.3	0.50	0.05	<0.02	<0.02	<0.02	0.13	0.02	101.8	72.2			
58	38.6	<0.01	0.02	24.13	38.6	0.46	0.09	<0.02	<0.02	<0.02	0.13	<0.01	102.1	74.0			
Pyroxene																	
C0009														Mg#	Wo	En	Fs
25	55.5	1.35	1.67	10.9	29.7	0.32	0.96	0.11	<0.02	<0.02	0.05	<0.01	100.6	82.9	3.2	80.2	16.6
26	55.6	1.24	1.45	10.9	29.7	0.32	0.99	0.09	0.04	<0.02	0.05	0.01	100.4	82.9	2.8	80.6	16.6
32	58.0	1.81	1.59	1.36	37.2	0.12	0.54	0.25	<0.02	<0.02	0.03	<0.01	100.9	98.0	2.9	95.1	2.0
39	58.8	1.19	0.52	1.11	38.2	0.05	0.49	0.19	<0.02	<0.02	0.04	<0.01	100.6	98.4	0.9	97.5	1.6
59	53.4	0.63	8.21	11.3	23.2	0.57	1.41	0.16	0.03	<0.02	0.08	0.31	99.2	78.5	16.7	65.4	17.9
Magnetite																	
A0029																	
84	0.06	<0.01	0.08	93.1	0.05	<0.02	0.07	<0.02	<0.02	<0.02	0.06	0.07	93.5				
87	0.15	0.01	0.07	92.8	0.08	0.05	0.07	<0.02	<0.02	<0.02	0.08	0.07	93.4				
A0037																	
118	0.48	0.01	0.15	92.6	0.07	0.09	0.05	0.05	<0.02	<0.02	0.05	0.03	93.6				
123	0.48	<0.01	0.17	92.0	0.07	0.15	0.05	0.21	<0.02	<0.02	0.06	0.10	93.3				
C0009																	
71	0.09	<0.01	0.04	93.0	0.06	0.04	0.06	<0.02	<0.02	<0.02	0.08	0.04	93.4				
73	0.29	<0.01	0.02	93.1	0.12	0.02	0.09	<0.02	<0.02	<0.02	0.07	0.05	93.7				
C0014																	
97	0.22	<0.01	0.02	93.4	0.02	0.04	0.09	0.05	<0.02	0.05	0.02	0.04	94.0				
100	0.16	0.03	0.14	93.2	0.03	0.03	0.06	<0.02	<0.02	<0.02	0.07	0.03	93.8				
C0068																	
109	0.51	0.03	0.08	91.9	0.23	0.02	0.08	<0.02	<0.02	<0.02	0.07	0.08	93.1				
114	0.06	0.01	0.05	92.8	0.02	<0.02	0.05	<0.02	<0.02	<0.02	0.03	0.03	93.0				

Ilmenite													
A0037													
131	0.29	0.02	0.49	37.1	0.17	9.25	0.33	50.51	<0.02	<0.02	0.08	0.06	98.3
C0009													
63	4.48	0.29	0.05	35.9	2.94	7.44	0.32	46.71	<0.02	<0.02	0.11	0.28	98.6
65	0.20	0.02	0.02	34.5	0.15	13.04	0.17	51.91	<0.02	<0.02	0.05	0.01	100.1
Spinel													
C0009													
66	0.34	61.5	0.27	0.86	23.3	0.02	0.26	0.43	0.24	<0.02	0.05	0.01	87.3

Supplementary Table 5. Chemical compositions (wt%) of phosphates determined by EPMA.

	P_2O_5	CaO	SiO_2	Na_2O	FeO	MgO	Cr_2O_3	MnO	SO_3	NiO	F	Cl	OH^*	Total	Fe+Cl eq	Total
Apatite																
A0037																
13	40.4	52.9	0.78	0.42	1.26	0.65	0.07	0.35	0.69	0.08	0.22	<0.01	3.16	97.8	-0.09	97.7
14	39.1	51.8	0.35	0.57	2.11	0.46	0.07	0.46	0.36	0.20	0.52	<0.01	2.78	96.0	-0.22	95.8
C0029																
17	39.3	52.0	0.71	0.85	1.07	0.62	<0.05	0.50	0.10	<0.07	0.09	<0.01	3.17	95.2	-0.04	95.2
18	40.1	53.0	0.65	0.56	1.07	0.45	<0.05	0.23	0.11	<0.07	0.73	<0.01	2.64	96.9	-0.31	96.6
Na-rich phosphate																
C0009																
25	20.7	0.03	13.0	5.68	8.64	21.0	0.25	<0.06	6.69	0.85	<0.08	0.14				79.9
26	23.9	0.04	11.6	6.66	8.08	21.0	0.18	0.10	5.93	0.55	<0.08	0.12				81.1

*OH content of the apatite was determined indirectly assuming that F + Cl + OH = 1.00 structural formula unit.

Supplementary Table 6. Chemical compositions of the Ryugu particles and selected carbonaceous chondrites (CI, CY) determined by LA-ICP-MS, normalized to Mg and CI values[14].

	A0029	C0068	Orgueil	Y-82162	Y 980115
Area (mm^2)	7.9×10^{-2}	1.5×10^{-2}	7.2×10^{-2}	5.4×10^{-2}	5.6×10^{-2}
Na	0.875	1.020	0.549	0.498	0.712
Mg	1.000	1.000	1.000	1.000	1.000
Al	0.918	1.026	1.125	1.060	1.007
Si	0.830	1.035	1.069	0.941	0.938
P	1.097	1.012	0.142	0.528	0.829
S	1.166	1.689	1.439	0.635	1.362
Cl	0.704	<0.66	<0.78	<0.51	<0.51
K	0.780	0.988	1.090	0.980	1.459
Ca	13.08	1.783	0.625	7.499	7.440
Sc	1.011	1.092	1.111	0.907	1.173
Ti	0.841	0.735	0.943	0.720	1.007
V	0.916	1.127	1.155	1.110	1.060
Cr	0.900	1.178	1.215	1.144	1.178
Mn	1.418	0.246	0.740	0.700	0.691
Fe	0.633	0.782	0.709	0.800	0.851
Co	0.907	1.436	1.152	0.861	1.057
Ni	0.742	1.205	0.914	0.719	0.912
Cu	0.611	0.628	0.842	1.061	0.816
Zn	0.940	1.770	1.686	0.210	1.098
Ga	0.944	1.129	1.093	0.762	1.067
Ge	0.988	1.303	1.215	0.664	1.288
As	0.940	1.462	1.378	0.882	1.205
Se	0.700	1.033	1.067	0.377	0.818
Rb	0.914	0.896	0.884	0.772	1.414
Sr	1.084	0.327	0.210	0.947	1.015
Y	0.887	0.403	0.482	0.803	0.822
Zr	0.855	1.280	1.061	0.974	1.174
Nb	1.041	1.038	1.022	0.983	1.435
Mo	1.404	1.494	1.150	1.480	1.362
Ru	0.852	1.225	1.090	0.914	1.160
Rh	1.119	1.583	1.379	1.200	1.454
Pd	0.904	1.471	1.230	1.477	1.374
Ag	1.075	1.614	1.460	0.655	2.034

Cd	0.508	1.713	1.395	<0.068	<0.054
In	1.145	1.941	1.634	<0.33	0.294
Sn	0.800	1.332	1.165	0.479	1.113
Sb	0.787	1.305	1.272	<0.60	1.080
Te	0.894	1.434	1.250	0.671	1.166
Cs	1.223	<0.72	0.929	<0.81	1.289
Ba	1.233	0.790	0.797	1.187	1.265
La	1.050	0.517	0.592	0.956	0.946
Ce	1.212	0.839	0.663	1.039	0.963
Pr	1.098	0.689	0.600	0.980	0.951
Nd	1.034	0.516	0.561	1.010	0.930
Sm	1.055	0.516	0.723	0.978	0.953
Eu	1.178	0.504	0.545	0.942	0.952
Gd	1.075	0.468	0.564	0.960	0.987
Tb	0.974	0.482	0.565	0.908	0.900
Dy	1.031	0.491	0.541	0.952	0.938
Ho	0.981	0.477	0.503	0.913	0.916
Er	1.048	0.514	0.558	0.974	0.968
Tm	1.028	<0.94	0.724	<0.95	0.945
Yb	1.043	0.537	0.606	0.985	1.021
Lu	1.043	0.539	0.654	0.977	1.053
Ta	<1.2	1.266	1.350	<1.2	<1.4
W	1.065	1.061	1.015	1.007	1.552
Re	0.916	1.382	1.192	1.263	1.101
Os	0.795	1.092	1.030	0.959	1.225
Ir	0.842	1.090	0.947	0.887	1.086
Pt	0.874	1.162	0.979	0.994	1.172
Au	0.867	0.541	1.030	0.981	2.160
Tl	0.893	1.651	1.113	0.043	<0.025
Pb	1.233	1.842	1.856	0.196	1.078
Bi	1.061	1.700	1.516	0.084	0.206
Th	0.683	0.631	0.724	1.228	1.044
U	1.161	0.942	0.993	1.458	1.161

Detection limits were defined by the average plus 3 standard deviation of background.

Reference

44. Piralla, M., Tartese R., Marrocchi, Y., & Joy, K.H. Apatite halogen and hydrogen isotope constraints on the conditions of hydrothermal alteration in carbonaceous chondrites. *Meteor. Planet. Sci.* **56,** 809-828. https://doi.org/10.1111/maps.13639 (2021)